Available online at www.sciencedirect.com
ScienceDirect
Thermochimica Acta 455 (2007) 134–137
thermochimica acta
www.elsevier.com/locate/tca

The solidus and liquidus temperatures of UO_2–Gd_2O_3 and UO_2–Er_2O_3 fuels

Ki Won Kang *, Jae Ho Yang, Jong Hun Kim, Young Woo Rhee, Dong Joo Kim, Keon Sik Kim, Kun Woo Song

Korea Atomic Energy Research Institute, Deokjin-dong 150, Yuseong-gu, Daejeon 305-353, Republic of Korea

Available online 2 December 2006

Abstract

The melting temperatures of UO_2–(4, 6, 8, 12) wt% Gd_2O_3, UO_2–(2, 4, 8) wt% Er_2O_3 and UO_2 fuels were measured. The fuels were prepared by sintering the green pellets of powder mixtures. Fuel fragments were loaded into a tungsten capsule filled with helium, and then they were melted by an induction heating. The melting temperature was measured by the thermal arrest method during a heating of the capsule. The solidus and liquidus temperatures of UO_2–Gd_2O_3 and UO_2–Er_2O_3 were also determined. The solidus temperatures of UO_2–Gd_2O_3 and UO_2–Er_2O_3 were almost 150–280 and 180–270 °C lower than their liquidus temperatures, respectively.

Keywords: Melting temperature; Thermal arrest; UO_2–Gd_2O_3; UO_2–Er_2O_3

1. Introduction

UO_2–Gd_2O_3 fuel is widely used as a burnable absorber in light water reactors. Gadolinium is a very strong neutron absorber and thus can reduce an excess reactivity in the first cycle of a reactor operation. The cycle length is currently about 15–18 months, and the Gd_2O_3 content ranges from 6 to 10 wt%, depending on the cycle length. An extension of the cycle length is one of the methods to increase the efficiency of reactor operation. For a longer cycle length, UO_2–Er_2O_3 is expected to be more adequate than UO_2–Gd_2O_3 since erbium is a less strong absorber.

The melting temperature of oxide fuel is one of the most important properties for estimating the behavior of a nuclear fuel during both a normal operation and postulated accident conditions. Since UO_2–$Gd(Er)_2O_3$ is a solid solution, UO_2–$Gd(Er)_2O_3$ fuel melts in a temperature range where Gd(Er) ions replace the U ions in the lattice. This fuel is produced by sintering a powder mixture of UO_2 with Gd_2O_3 or Er_2O_3. The melting of UO_2–$Gd(Er)_2O_3$ begins at the solidus temperature and ends at the liquidus temperature.

Beals et al. [1] reported that the solidus temperature of UO_2–Gd_2O_3 was 300–400 °C lower than the liquidus temperature. However, Wada et al. [2] found that the solidus temperature was very close to the liquidus temperature although they did not measure the solidus temperature quantitatively. Thus, there is a big difference between the known solidus temperatures of UO_2–Gd_2O_3.

UO_2–Er_2O_3 fuel is expected to have 1–2 wt% Er_2O_3. The solidus and liquidus temperatures have not been known until now. Therefore, we need more data to understand the melting points of UO_2–Gd_2O_3 and UO_2–Er_2O_3 fuels. This paper reports the solidus and liquidus temperatures of UO_2–Gd_2O_3 and UO_2–Er_2O_3 fuels.

2. Experimental

Fuel materials used in the melting experiment were UO_2–(4, 6, 8, 12) wt% Gd_2O_3 and UO_2–(2, 4, 8) wt% Er_2O_3 fuels. Fuel materials were fragments of sintered pellets, which were produced at 1730 °C in a H_2–3% H_2O gas atmosphere. About 18 g of each fuel fragment was loaded into a tungsten capsule which was filled with helium after evacuated down to 10^{-2} Torr. The capsule was sealed by welding and a helium leak test was implemented to prove that the capsule had no leaks.

The tungsten capsule is a cylinder with 16 mm in diameter and 42 mm in height, and the upper lid of the capsule has

* Corresponding author.
E-mail address: kwkang@kaeri.re.kr (K.W. Kang).

0040-6031/$ – see front matter © 2006 Published by Elsevier B.V.
doi:10.1016/j.tca.2006.11.027

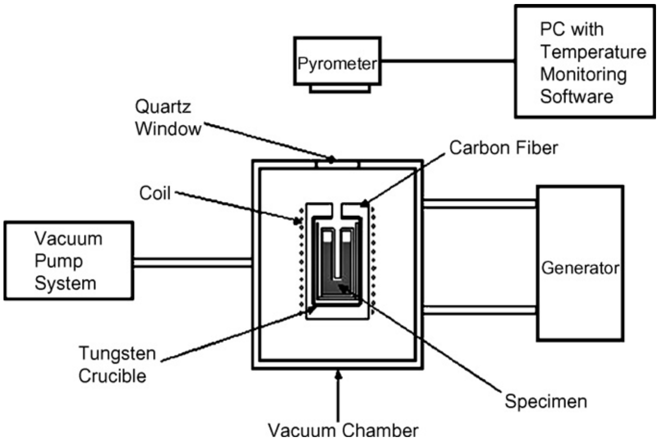

Fig. 1. Schematic diagram of the apparatus for measuring the melting temperature.

a one end sealed tube extended into the inside of the capsule. This tube can provide the black body condition for a measurement of the temperature. Fig. 1 shows a schematic diagram of an apparatus for measuring the melting temperature. The capsule was surrounded by tungsten susceptor, carbon fiber and an induction coil, in that order. This arrangement was placed in a chamber, which was evacuated below 10^{-4} Torr and then purged by Ar gas. The capsule was heated by an induction generator, which has a capacity of 30 kW operating at a frequency of 60 kHz. During a heating of the capsule, the fuel temperature was continuously measured in the black body hole by using a two-color pyrometer mounted on the chamber.

The power for a heating of the capsule was steadily increased to a certain power by using a computer program. Then, the fuel temperature was increased in accordance with the power. The melting temperature was determined as the temperature at which the increase of the temperature was arrested by the heat of the fusion.

The temperature obtained by the pyrometer was calibrated against the known melting points of the materials such as Gd_2O_3 and Nd_2O_3. Fig. 2 shows an example of the temperature–time profile for the Gd_2O_3 melting point. A thermal arrest appeared at 2428 °C which is close to the known melting temperature of 2420 °C for Gd_2O_3.

With one capsule containing a fuel, we measured the melting point several times by repeating a heating and cooling without a capsule failure. In this case the differences between the melting points were well within the range of ±10 °C. Even if the same material was melted in new capsules with a new alignment of the pyrometer, the melting point was changed. But the differences of all the measured melting points of the same material were in the range of ±20 °C. So the uncertainty of the melting point is believed to be ±20 °C. This uncertainty does not have any statistical significance but simply represents a conservative estimate of the maximum error derived from an experimental error and an instrumental bias. The solidus temperature is difficult to read from the temperature–time curve because of a blunt change in the curve at that temperature. The uncertainty associated with the solidus temperature is considered to be as large as ±25 °C.

3. Results and discussion

Fig. 3 shows one example of the typical temperature–time profiles for the determination of the UO_2–8 wt% Er_2O_3 fuel. The slope of the temperature increase shows a slowdown in the range between 2500 and 2600 °C and a typical thermal arrest appeared in the vicinity of 2797 °C. The UO_2–8 wt% Er_2O_3 fuel is a solid solution and thus it has both solidus and liquidus temperatures. The solidus temperature (T_S), the start of a melting, can be identified by a decrease in the temperature slope, and the liquidus temperature (T_L), the end of a melting, can be identified by an increase in the temperature slope. Solidus and liquidus temperatures of fuel specimens are obtained from the first and second indications of change in slope of the heating curve [3,4].

The arrows in Fig. 3 indicate the T_S and T_L. The solidus temperature is more difficult to determine than the liquidus temperature since the change in the temperature slope is very small.

The temperature–time profiles of the UO_2–(2, 4) wt% Er_2O_3 fuel are similar to Fig. 3. The solidus and liquidus temperatures

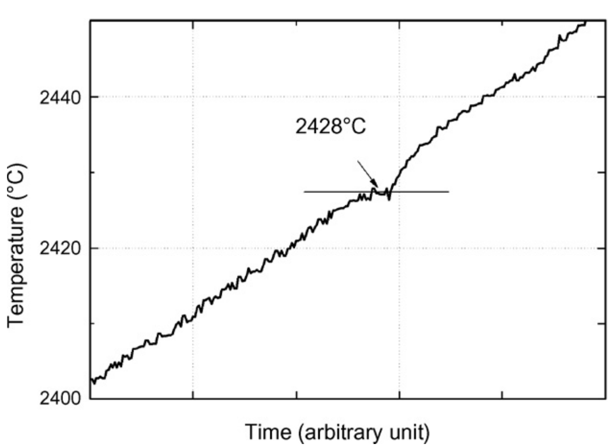

Fig. 2. A temperature–time plot showing the melting point of Gd_2O_3 as a reference sample.

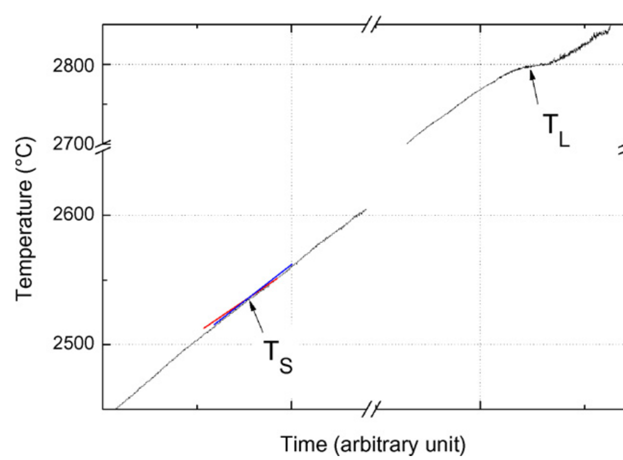

Fig. 3. A temperature–time plot showing the solidus and liquidus temperatures of UO_2–8 wt% Er_2O_3 by the thermal arrest method.

Table 1
The solidus and liquidus temperatures of UO_2–Gd_2O_3 and UO_2–Er_2O_3

Material	Melting temperature (°C)	
	T_S	T_L
UO_2–4 wt% Gd_2O_3	2670 ± 25	2820 ± 20
UO_2–6 wt% Gd_2O_3	2620 ± 25	2818 ± 20
UO_2–8 wt% Gd_2O_3	2537 ± 25	2783 ± 20
UO_2–12 wt% Gd_2O_3	2461 ± 25	2739 ± 20
UO_2–2 wt% Er_2O_3	2635 ± 25	2822 ± 20
UO_2–4 wt% Er_2O_3	2600 ± 25	2790 ± 20
UO_2–8 wt% Er_2O_3	2532 ± 25	2797 ± 20

are determined and shown in Table 1. The liquidus temperature decreases slightly with the Er_2O_3 content, but the solidus temperature decreases more significantly than the liquidus temperature. The solidus temperatures which depend on the Er_2O_3 content are about 180–270 °C lower than the liquidus temperatures.

Fig. 4 shows an example of the temperature–time profiles for the UO_2–6 wt% Gd_2O_3 fuel. The arrows indicate the solidus and liquidus temperatures. The liquidus temperature can be determined more clearly than the solidus temperature. The solidus and liquidus temperatures are shown in Table 1 and they are plotted in Fig. 5 together with other data [1,2].

Fig. 5 shows that the liquidus temperatures range between 2820 and 2739 °C for UO_2–(4, 6, 8, 12) wt% Gd_2O_3 and thus are 30–110 °C lower than the melting point of UO_2. Our liquidus temperatures of UO_2–(4, 6, 8, 12) wt% Gd_2O_3 are almost linearly decreased as the Gd_2O_3 content is increased. The liquidus temperature of Wada et al. [2] also exhibits nearly the same dependency of the Gd_2O_3 content. However, Beals et al. [1] have shown a different dependency of the liquidus temperature on the Gd_2O_3 content; it is increased considerably by an increase in the Gd_2O_3 content from 7 to 14 wt%. Our liquidus temperatures are almost linearly decreased as the Gd_2O_3 content is increased, slightly higher than the other data.

Fig. 5 shows that the solidus temperatures of UO_2–Gd_2O_3 are 150–280 °C lower than the liquidus temperatures. Wada et al. [2], from many observations, found that the solidus temperature lies very close to the liquidus temperature while Beals et al. [1] have reported that the solidus temperature is 300–400 °C lower than the liquidus temperature. Therefore, our solidus temperatures lie between the two reported values [1,2].

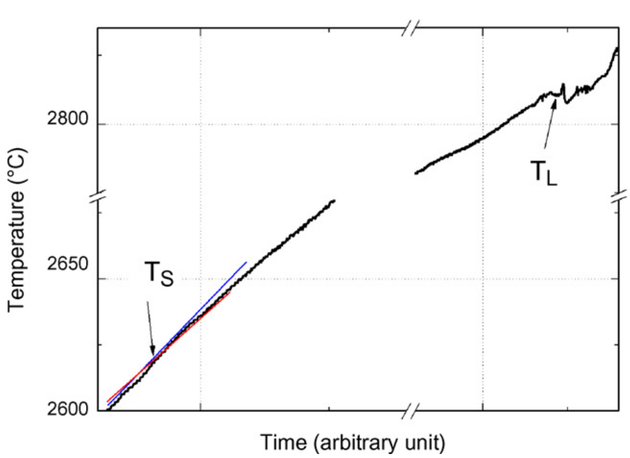

Fig. 4. A temperature–time plot showing the solidus and liquidus temperatures of UO_2–6 wt% Gd_2O_3 by the thermal arrest method.

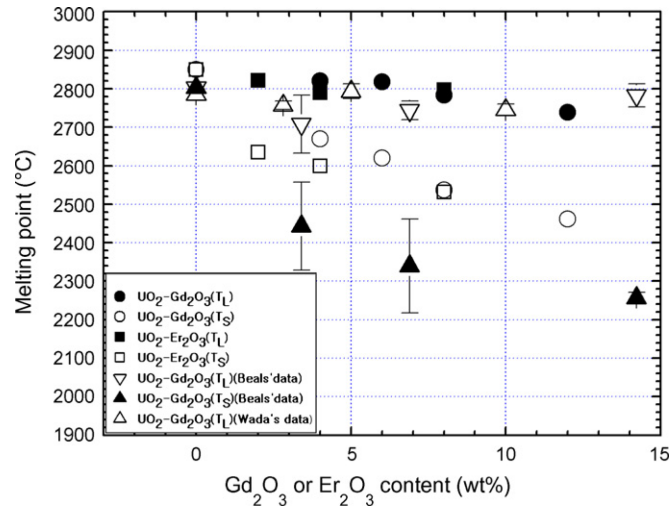

Fig. 5. The melting points of UO_2–Gd_2O_3, UO_2–Er_2O_3 and UO_2 fuels.

Table 2
Comparison of the melting temperature of UO_2 with other data

References	Melting point (°C)
Lyon et al. [5]	2840 ± 20
Latta et al. [6]	2865 ± 15
Tachibana et al. [4]	2845 ± 25
Carbajo et al. [7]	2847 ± 30
This work	2850 ± 20

The melting point of UO_2 is also determined as 2850 ± 20 °C. There are lots of other data about the melting point of unirradiated UO_2 measured by the thermal arrest method as summarized in Table 2 [4–7]. Our melting point of UO_2 is in good agreement with the other data.

4. Conclusion

The melting points of UO_2–Er_2O_3, UO_2–Gd_2O_3 and UO_2 were measured by the thermal arrest method. The melting point of UO_2 is 2850 ± 20 °C. The liquidus temperature of UO_2–Er_2O_3 decreases with the Er_2O_3 content, and the solidus temperatures are about 180–270 °C lower than the liquidus temperatures. The liquidus temperatures of UO_2–(4, 6, 8, 12) wt% Gd_2O_3 are about 30–110 °C lower than the UO_2 melting point. It is found that the solidus temperatures of UO_2–(4, 6, 8, 12) wt% Gd_2O_3 are almost 150–280 °C lower than the liquidus temperatures.

Acknowledgement

This work has been carried out under the Nuclear R&D Program supported by the Ministry of Science and Technology in Korea.

References

[1] R.J. Beals, J.H. Handwerk, B.J. Wrona, J. Am. Ceram. Soc. 52 (1969) 578.
[2] T. Wada, K. Noro, K. Tsukui, Behavior of UO_2–Gd_2O_3 fuel, in: BNES Nuclear Fuel Performance, 1973, p. 63.1.
[3] J. Komatsu, T. Tachibana, K. Konashi, J. Nucl. Mater. 154 (1988) 38.
[4] T. Tachibana, T. Ohmori, S. Yamanouchi, T. Itaki, J. Nucl. Sci. Technol. 22 (1985) 155.
[5] W.L. Lyon, W.E. Baily, J. Nucl. Mater. 22 (1967) 332.
[6] R.E. Latta, R.E. Fryxell, J. Nucl. Mater. 35 (1970) 195.
[7] J.J. Carbajo, G.L. Yoder, S.G. Popov, V.K. Ivanov, J. Nucl. Mater. 299 (2001) 181.